



Effect of the Synthesis Time on Structural Properties of Copper Oxide

Karrar A. Alsoltani

Department of Physics, College of Education
for Pure Science Ibn Al-Haitham, University of
Baghdad, Baghdad-Iraq.

karrar.Ameen1104a@ihcoedu.uobaghdad.edu.iq

Khalid H. Harbbi

Department of Physics, College of Education
for Pure Science Ibn Al-Haitham, University of
Baghdad, Baghdad-Iraq.

Khalid@ircoedu.uobaghdad.edu.iq

Article history: Received 21 September 2022, Accepted 17 October 2022, Published in April 2023.

doi.org/10.30526/36.2.3024

Abstract

the structural properties of the CuO nanopowder oxide prepared reflux technique without any templates or surfactant, using copper nitrate hydrate ($\text{Cu}(\text{NO}_3)_2 \cdot 3\text{H}_2\text{O}$) in deionized water with aqueous ammonia solution are reported. The Xrd analysis data and processing in origin pro program used to get FWHM and integral width to study the effect of different synthesis times was studied on the structural properties. It was found that values of crystal sizes are 17.274nm, 17.746nm, and 18.560nm, the size of nanoparticles is determined by Halder-Wagner, and 15.796 nm, 15.851nm, and 16.52nm, were calculated by Size-Strain Plot (SSP) method. The Sample was considered to determine physical and microstructural parameters such as internal strain, dislocations density, surface area, and the number of unit cells and then to compare the results.

Keywords: CuO, Originpro, Xrd, Halder-wagner, Size-strain plot .

1. Introduction

In the past few decades, nanoparticles of a variety of sizes, shapes, and compositions, have been found, their physical and chemical properties attract the current scientific field over bulk materials [1]. Quite possibly of the main boundary in the combination of these nanoparticles is the control of molecule size, morphology, and crystallinity and to accomplish this objective, so were developed different synthesis methods ; some of the most investigated approaches include the sonochemical , sol-gel method, laser removal, the electrochemical , substance precipitation and surfactant-based procedures [2]. Nanostructured transition metal oxides have attracted considerable attention from researchers in recent years [3]. Copper (II) oxide, CuO, also known as cupric oxide has drawn in much consideration lately due to its promising applications as CuO is an appealing p-type metal oxide semiconductor that has extraordinary electrical, optical and synergist properties, solar-cells, and sensors espithaly gas type. [4-7]. Copper oxide is a compound of two elements, copper and oxygen, which are d and p block elements in the periodic table respectively. In a crystal, the copper ion is coordinated by four oxygen ions [8]. (CuO) is has a

monoclinic construction and is a special monoxide compound for both essential examinations and commonsense applications [9]. The lattice parameters are $a = 4.6850 \text{ \AA}$, $b = 3.4230 \text{ \AA}$ and $c = 5.1320 \text{ \AA}$ [10]. In this work nanopowder of CuO was prepared at different synthesis times. Samples for different of synthesis times 6hours, 12hours, and 24hours have studied the effect of synthesis times on the structural parameters by studying X-ray diffraction (XRD) and comparing and discussing the result.

2. Theory

• Method of Halder-Wagner

In the method of Halder-Wagner where strain and crystallite size profiles are described by Gauss and Lorentzian [11].

$$\left(\frac{\beta_{hkl}^*}{d_{hkl}^*}\right)^2 = \left(\frac{1}{D}\right) \left(\frac{\beta_{hkl}^*}{d_{hkl}^*}\right) + \left(\frac{\varepsilon}{2}\right)^2 \quad (1)$$

Where, $\beta_{hkl}^* = \beta \cos \theta / \lambda$ and $d_{hkl}^* = 2 \sin \theta / \lambda$ and λ the wavelength of the X-ray plot was $\left(\frac{\beta_{hkl}^*}{d_{hkl}^*}\right)^2$ against $\left(\frac{\beta_{hkl}^*}{d_{hkl}^*}\right)$ is a straight line. The mean diameter was obtained by the inverse slope of the line, while the strain distortions are obtained from y-intercept [12,13].

• Size-strain Plot Method

This method is an advantage that peaks in the low and middle angle ranges are given more weight as overlap between the diffraction peaks are much less. According to the process of size-strain plot, the relationship between lattice strain and crystal size is given by [14]

$$(d_{hkl} \beta_{hkl} \cos \theta)^2 = \left(\frac{K}{D}\right) (d_{hkl}^2 \beta_{hkl} \cos \theta) + (2\varepsilon)^2 \quad (2)$$

Where $(\beta_{hkl} / d_{hkl})^2$ represents X axis and $(\beta_{hkl} / d_{hkl}^2)^2$ represents Y axis. The mean crystal size value is calculated from the slope while the intersection gives the strain ε .

3. Results and Discussion

According to XRD patterns of Copper Oxide (CuO) NNPs developed on copper foils for various syntheses, times are shown in Figure1. Were observed different peaks at $(2\theta) = 31.19^\circ$ (110), 34.72° (002), 38.51° (111), 50.48° (-202), 56.26° (020), 62.03° (202), 66.12° (-113), 71.94° (-311) and 74.23° (220) relates to various planes of the monoclinic phase of CuO [15], shows in situ for samples 1-3. Through a program (WebPlotDigitizer-4.5), we obtain data for intensity and 2θ of CuO nanoparticles to all profile lines with nine peaks.

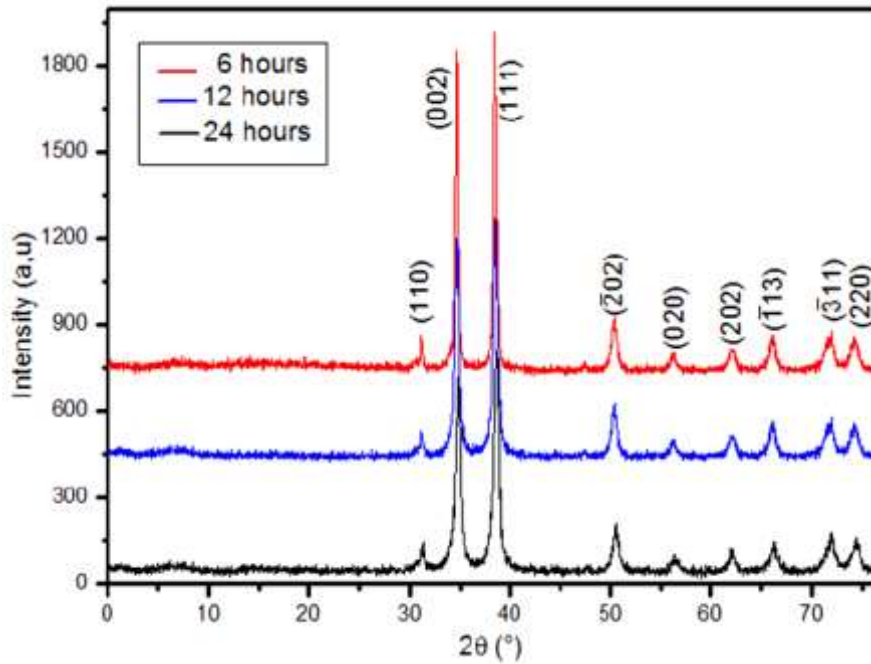


Figure1. XRD patterns of CuO NPs prepared at different synthesis times. [15]

In addition, this data is used to draw the shape of the peaks using an analytical program (Origin Pro Lab) to calculate the area under the curve and the FWHM is calculated by the program and then calculate integral breadth was the integral breadth which is [16]:

$$\beta = A / I_0 \tag{3}$$

Where A was the area under the curve and the I_0 was the highest intensity of the peak for each sample and for the different peaks respectively.

By processing the data used Originpro to get the below Figures and tables. Through these results, the above equations will be applied to calculate each of the crystal sizes and strains by the above methods in order to distinguish the effect of synthesis times on it.

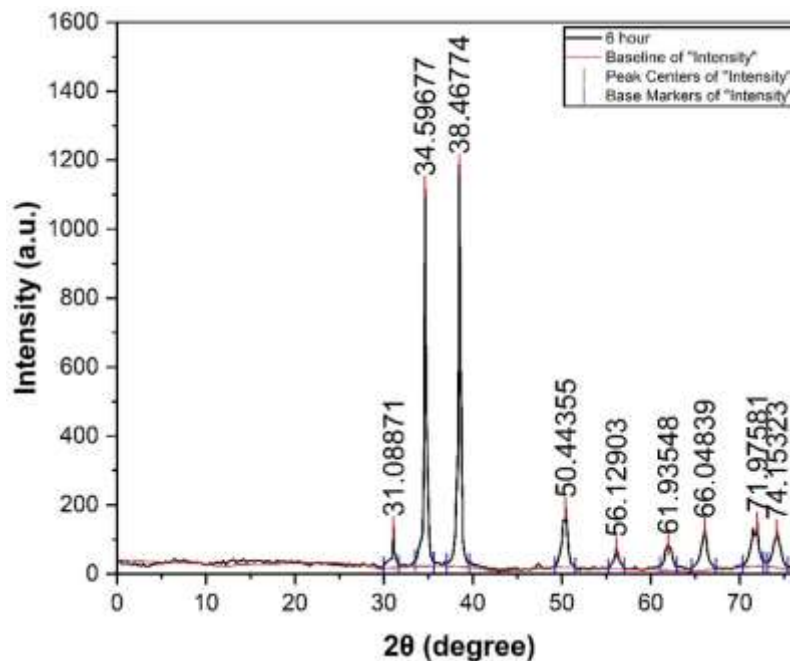


Figure2. XRD patterns of CuO NPs prepared at 6 hour synthesis time by Originpro.

Table 1. result of CuO NPs prepared at 6 hours by Originpro.

(h k l)	2θ	Area	FWHM	Height	β
(1 1 0)	31.089	13.235	0.104	118.134	0.112
(0 0 2)	34.597	272.214	0.246	1101.241	0.247
(1 1 1)	38.468	395.599	0.338	1166.384	0.339
(-2 0 2)	50.444	109.108	0.628	172.221	0.634
(0 2 0)	56.129	24.198	0.371	62.571	0.387
(2 0 2)	61.935	53.185	0.696	74.966	0.709
(-1 1 3)	66.048	76.801	0.624	121.415	0.633
(-3 1 1)	71.976	120.136	0.942	126.479	0.95

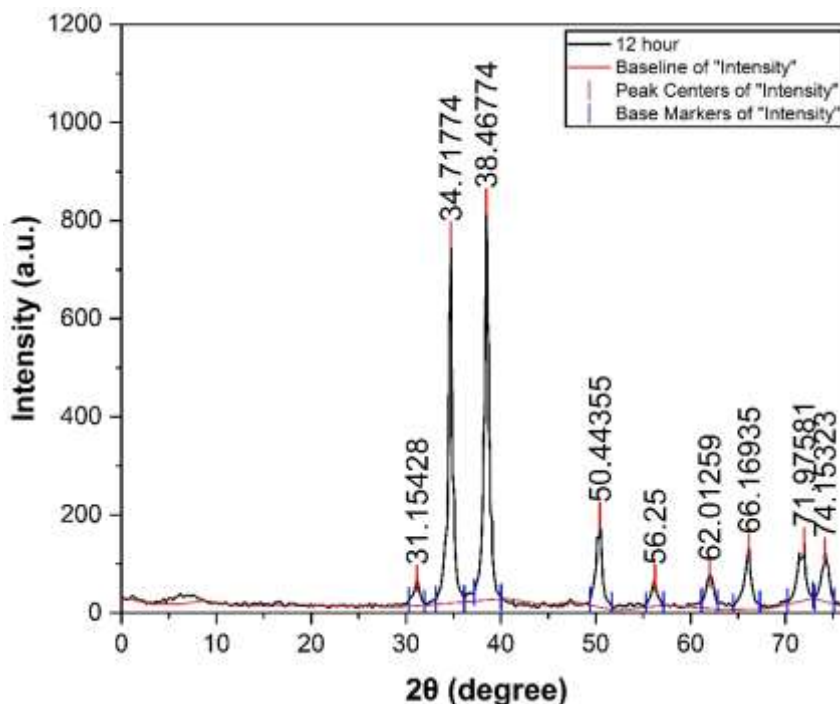


Figure3. XRD patterns of CuO NPs prepared at 12 hour synthesis time by Originpro.

Table 2. result of CuO NPs prepared at 12 hours by Originpro.

(h k l)	2θ	Area	FWHM	Height	β
(1 1 0)	31.154	32.701	0.563	56.325	0.581
(0 0 2)	34.718	466.623	0.62	750.63	0.622
(1 1 1)	38.468	400.479	0.492	812.328	0.493
(-2 0 2)	50.444	124.019	0.659	186.672	0.664
(0 2 0)	56.25	32.861	0.549	58.027	0.566
(2 0 2)	62.013	52.383	0.735	69.919	0.749
(-1 1 3)	66.169	88.908	0.693	126.774	0.701
(-3 1 1)	71.976	127.039	1.031	122.195	1.04

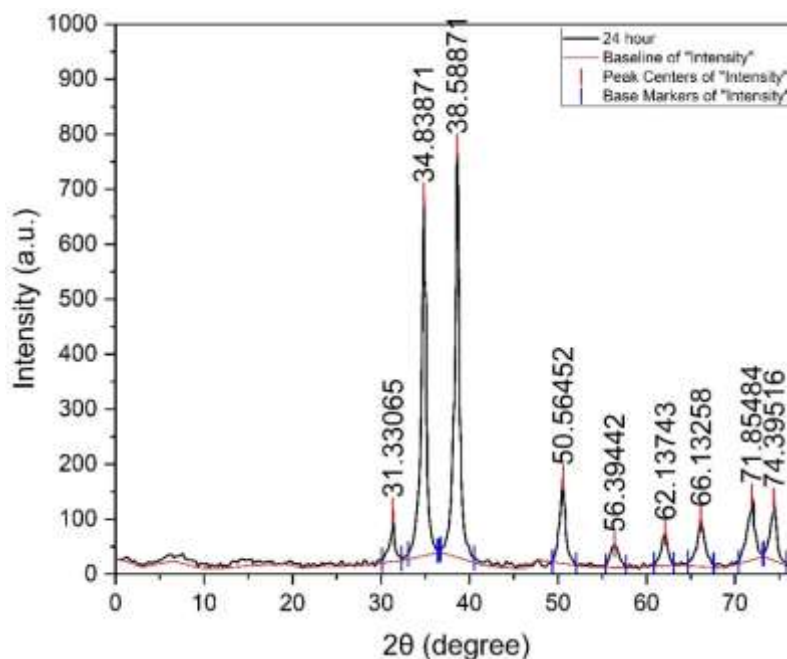


Figure4. XRD patterns of CuO NPs prepared at 24 hour synthesis time by Originpro.

Table 3. result of CuO NPs prepared at 24 hours by Originpro.

(h k l)	2θ	Area	FWHM	Height	β
(1 1 0)	34.839	50.105	0.524	93.699	0.535
(0 0 2)	38.589	427.655	0.651	655.394	0.653
(1 1 1)	50.565	472.581	0.631	747.106	0.633
(-2 0 2)	56.394	119.626	0.759	156.365	0.765
(0 2 0)	62.137	32.325	0.754	41.566	0.778
(2 0 2)	66.133	37.797	0.647	59.963	0.63
(-1 1 3)	71.855	72.658	0.847	86.946	0.836
(-3 1 1)	74.395	126.554	1.097	116.241	1.089

Determination of crystallite size and the lattice strain

Halder-Wagner method

After calculating the integral breadth of all peaks for all three samples then we use equations $\beta_{hkl}^* = \beta \cos \theta / \lambda$ and $d_{hkl}^* = 2 \sin \theta / \lambda$ where λ is the wavelength of the X-ray (0.15046) and plot $(\frac{\beta_{hkl}^*}{d_{hkl}^*})^2$ against $(\frac{\beta_{hkl}^*}{d_{hkl}^*})$ then fitting the data by a straight line to compare with eq (1) by getting straight line equation to obtained crystallite size and the lattice strain. The results are shown in Table (4).

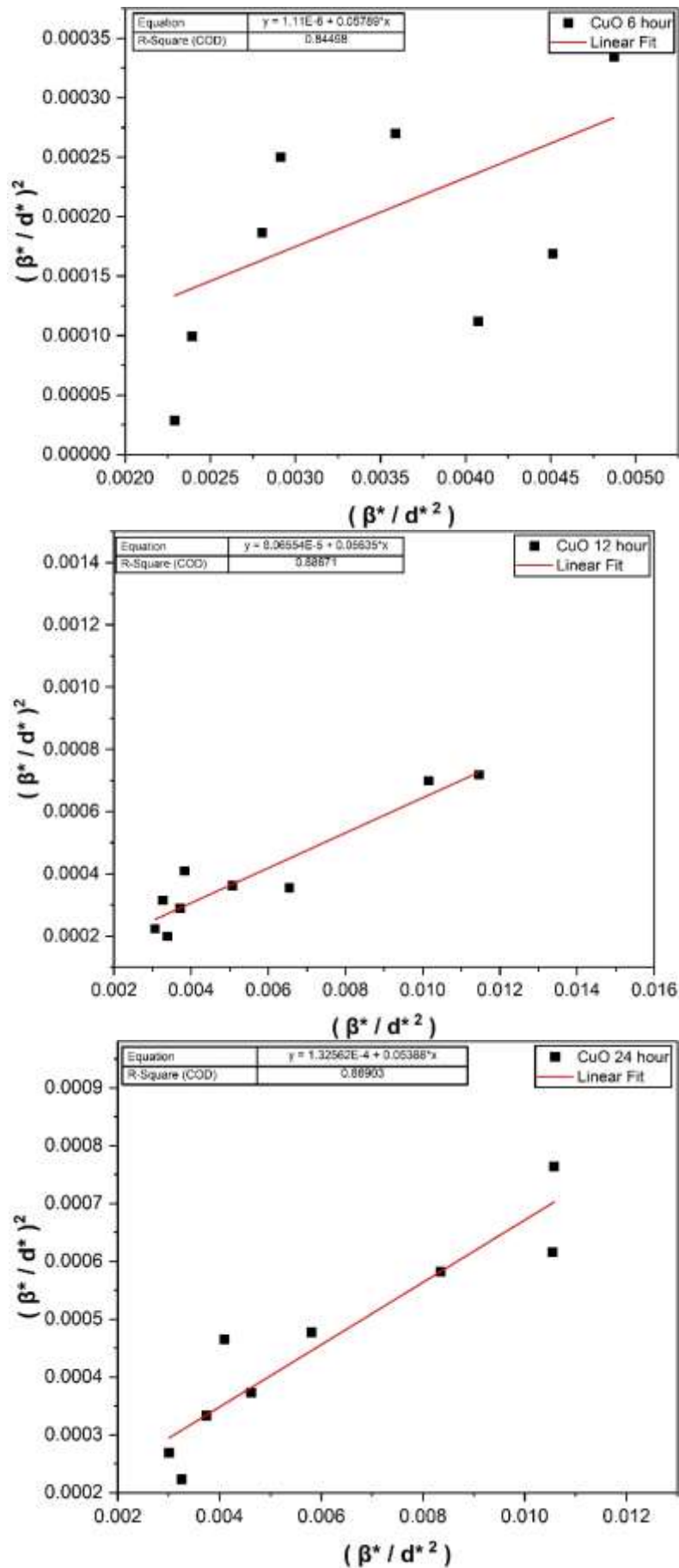


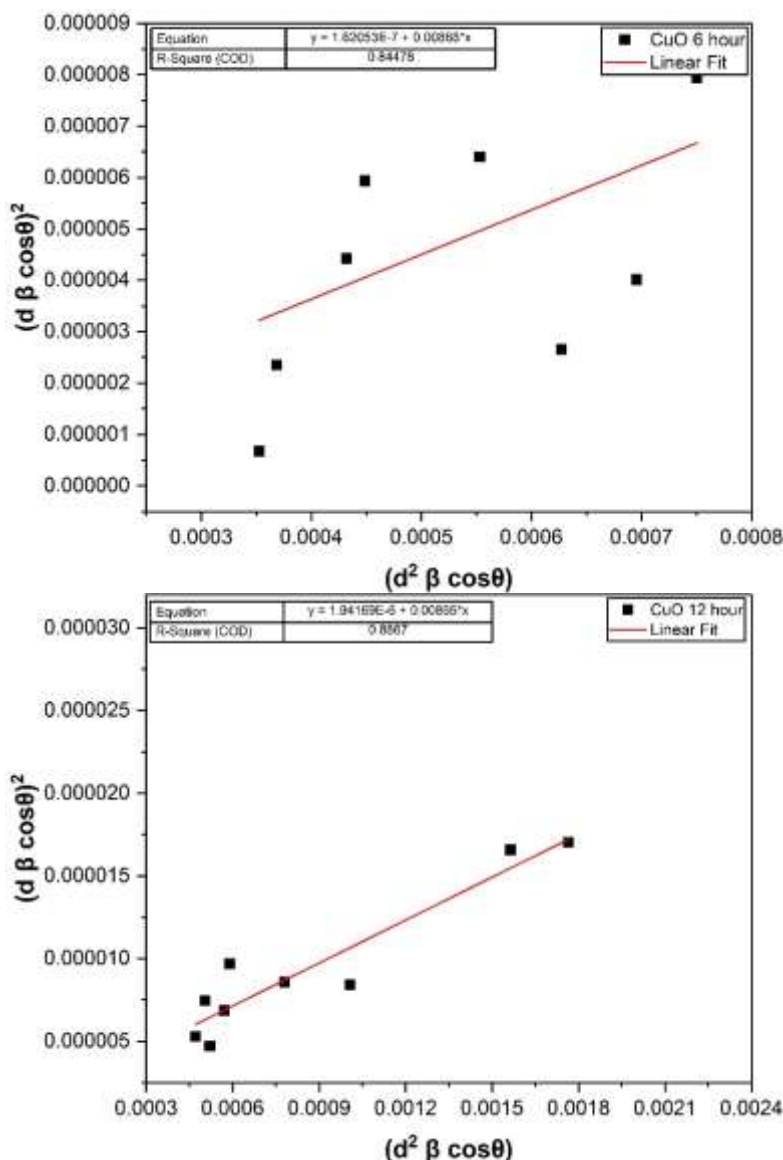
Figure 5. Halder-Wagner method for each sample respectively.

Table 4. result of crystallite size and the lattice strain by Halder-Wagner method for all CuO NPs sample

Time hours	D nm	ϵ strain
CuO 6 hour	17.274	0.002
CuO 12 hour	17.746	0.018
CuO 24 hour	18.560	0.023

Size-strain plot method

Equation (2) In this method is used to calculate particle size for each diffraction line and Equation (2) represents Where $(\beta_{hkl} / d_{hkl})^2$ represents X-axis and $(\beta_{hkl} / d_{hkl}^2)^2$ represents Y-axis and $d_{hkl}^2 B_{hkl} \cos\theta$ calculated in radians and uses a wavelength of X-ray equal to 0.15046 as shown in figure 6, we can see in this method inverse relationship between crystal size and strain. The results were calculated and included in Table (5).



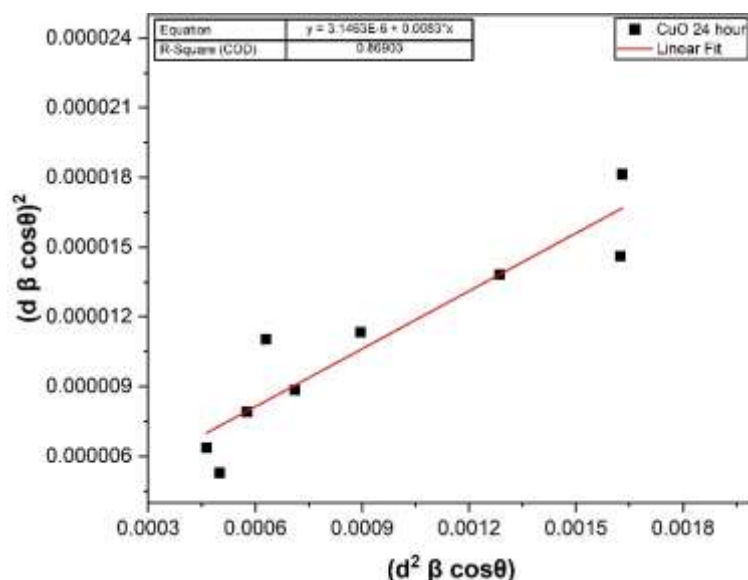


Figure 6. Size-strain plot method for each sample respectively

Table 5. result of crystallite size and the lattice strain Size-strain plot method for all CuO NPs sample

Time hours	D nm	ε strain
CuO 6 hour	15.796	0.001
CuO 12 hour	15.851	0.003
CuO 24 hour	16.52	0.004

The surface area (S.A) can be calculated by the following equation [17]:

$$S.A=6 \cdot 10^3 / D \rho \tag{3}$$

From XRD we can calculate the x-ray density of powder by using this equation [18]:

$$\rho = Z \text{ Mwt} / V \text{ Na} \tag{4}$$

Where ρ: density (g/cm³), Mwt: molar mass 79.545 (g/mol) for CuO, Z: the number of atoms: unit cell volume (cm³), and Na: Avogadro number (1/mol) [19].

The dislocation density (δ) and the number of unit cells (n) are calculated using the following relations [20,21]:

$$\delta = 1 / D^2 \tag{5}$$

$$n = \pi D^3 / 6 V \tag{6}$$

Their calculated values will be presented in table 6.

Table 6. Shows lattice parameter, X-ray and dislocations density, surface area, and number of unit cells for all CuO NPs sample.

sample	CuO for 6 hours	CuO for 12 hours	CuO for 24 hours
S.A (m ² /g)	55.046	53.582	51.232
δ(1/m ²) *10 ¹⁵	3.351	3.175	2.902
n	33928.49	36786.39	42084.26

4. Conclusions

We review the current knowledge about CuO and added new experimental and theoretical results which provide a better understanding of the structure and effect of Synthesis time. Increased preparation time saw that all plane peaks of CuO are marginally moved to higher angles indicating a little decrease in the size, more essential to notice the lower peak intensity is particularly in the case of prepared CuO in 24hours. The change nanoparticles size depends on the synthesis time. However, the size of particles increases by increasing Synthesis times, dislocation density, and specific surface area decreases as increasing preparation times. The number of unit cells steadily increases with time. These current perceptions can assist with working on how we might our understanding of physical properties and the formation of CuO nanoparticles. When comparing the two analysis methods that were used in this study noticed that the Halder-Wagner method gave high accuracy in results, because the equations used in this method put points in locations as close as possible to the straight line in the diagram. There is a convergence in the results of the Halder-Wagner method with the results of the ssp methods, and the two methods are also close because the results are within the nanoscale.

References

1. Wang, X.; Zhuang, J.; Peng, Q.; Li, Y.; WANG, Xun.; et al. A general strategy for nanocrystal synthesis. *Nature*, **2005**, *437*.7055 121-124.
2. Grigore, M. E.; Biscu, E. R.; Holban, A. M.; Gestal, M. C.; Grumezescu, A. M. Methods of synthesis, properties and biomedical applications of CuO nanoparticles. *Pharmaceuticals*, **2016**, *9*.4, 75.
3. Narayan, H.; Alemu, H.; Jaybhaye, S. Copper Oxide Nanoparticles: Synthesis and Characterization. Proceedings of the AATMC-2018, *Kalyan, India*, **2018**, 43-47.
4. Dindar, A.; Kim, J. B.; Fuentes-Hernandez, C.; Kippelen, B. Metal-oxide complementary inverters with a vertical geometry fabricated on flexible substrates. *Applied Physics Letters*, **2011**, *99*.17, 172104.
5. Sahay, R.; Sundaramurthy, J.; Kumar, P.S.; Thavasi, V.; Mhaisalkar, S.G.; Ramakrishna, S. Synthesis and characterization of CuO nanofibers, and investigation for its suitability as blocking layer in ZnO NPs based dye sensitized solar cell and as photocatalyst in organic dye degradation. *Journal of Solid State Chemistry*, **2012**, *186*, 261-267.
6. Gao, S.; Yang, S.; Shu, J.; Zhang, S.; Li, Z.; Jiang, K. Green fabrication of hierarchical CuO hollow micro/nanostructures and enhanced performance as electrode materials for lithium-ion batteries. *The Journal of Physical Chemistry C*, **2008**, *112*.49, 19324-19328.
7. Comanac, A.; de'Medici, L.; Capone, M.; Millis, A. J. Optical conductivity and the correlation strength of high-temperature copper-oxide superconductors. *Nature Physics*, **2008**, *4*.4, 287-290.
8. Guajardo-Pacheco, M. J.; Morales-Sánchez, J. E.; González-Hernández, J.; Ruiz, F. Synthesis of copper nanoparticles using soybeans as a chelant agent. *Materials letters*, **2010**, *64*.12, 1361-1364.
9. Rajagopalan, S.; Koper, O.; Decker, S.; Klabunde, K. J. Nanocrystalline metal oxides as destructive adsorbents for organophosphorus compounds at ambient temperatures. *Chemistry—A European Journal*, **2002**, *8*.11, 2602-2607.

10. File, P. D.; JCPDS-ICDD, 12 Campus Boulevard. *Newtown Square, PA*, **2001**, 247: 19073-3273.
11. Kamil, M. K.; Jasim, K. A. Investigation the Crystalline Size and Strain of Perovskite (YBa₂Cu₃O₆) by variant method. *Test Engineering and Management*, **2020**, 8719, 8719-8723.
12. sadiq Khasro, F.; Mahmood, H.S. Enhancement of Antibacterial Activity of Face Mask with Gold Nanoparticles. *Ibn AL-Haitham Journal For Pure and Applied Sciences*, **2022**. 35(3), 25-31.
13. Kamil, M. K.; Jasim, K. A. Calculating of crystalline size, strain and Degree of crystallinity of the compound (HgBa₂Ca₂Cu₃O₈+ σ) by different method. In: IOP Conference Series: *Materials Science and Engineering*. IOP Publishing, **2020**, 072109.
14. Rabiei, M.; Palevicius, A.; Monshi, A.; Nasiri, S.; Vilkauskas, A.; Janusas, G. Comparing methods for calculating nano crystal size of natural hydroxyapatite using X-ray diffraction. *Nanomaterials*, **2020**, 10.9: 1627.
15. Bouazizi, N.; Bargougui, R.; Oueslati, A.; Benslama, R. Effect of synthesis time on structural, optical and electrical properties of CuO nanoparticles synthesized by reflux condensation method. *Advanced materials letters*, **2015**, 6.2: 158-164.
16. Langford, J. I. The use of the Voigt function in determining microstructural properties from diffraction data by means of pattern decomposition. *NIST Spec. Pub*, **1992**, 846: 110-126.
17. Antony, J.; Nutting, J.; Baer, D. R.; Meyer, D.; Sharma, A.; Qiang, Y. Size-dependent specific surface area of nanoporous film assembled by core-shell iron nanoclusters. *Journal of Nanomaterials*, 2006, **2006**.
18. Musa, K. H. Investigating the Structural and Magnetic Properties of Nickel Oxide Nanoparticles Prepared by Precipitation Method. *Ibn Al-Haitham Journal For Pure and Applied Sciences*, **2022**, 35(4).
19. RAMANATHAN, C.; SUBRAMANIAN, S.; VALANTINA, R. Structural and electronic properties of CuO, CuO₂ and Cu₂O Nanoclusters—a DFT approach. *Materials science*, **2015**, 21.2, 173-178.
20. Gaber, A.; Abdel-Rahim, M. A.; Abdel-Latif, A. Y.; Abdel-Salam, M. N. Influence of calcination temperature on the structure and porosity of nanocrystalline SnO₂ synthesized by a conventional precipitation method. *Int J Electrochem Sci*, **2014**, 9.1, 81-95.
21. Singh, P.; Kumar, A.; Kaushal, A.; Kaur, D.; Pandey, A.; Goyal, R. N. In situ high temperature XRD studies of ZnO nanopowder prepared via cost effective ultrasonic mist chemical vapour deposition. *Bulletin of Materials Science*, **2008**, 31.3, 573-577.